Stochastic instability of classical homogeneous $SU(2) \otimes U(1)$ fields with spontaneously broken symmetry

G. P. Berman, Yu. I. Man'kov, and A. F. Sadreev

Kirenskiĭ Institute of Physics, Siberian Division of the Academy of Sciences of the USSR
(Submitted 28 May 1984)
Zh. Eksp. Teor. Fiz. **88**, 705–714 (March 1985)

Classical homogeneous $SU(2) \otimes U(1)$ fields with a spontaneously broken symmetry are analyzed numerically, and the region of energies corresponding to stochastic motion is determined. The frequency spectrum of massive and massless fields is calculated for dynamic and stochastic motion.

INTRODUCTION

The Yang-Mills gauge fields[1] currently play a leading role in elementary particle physics, and there is much interest both in the quantization of Yang-Mills (YM) fields and in the characteristic features of their dynamic behavior.[2–6] In this connection we may mention the stochastic behavior of classical homogeneous YM fields that was recently discovered in Refs. 7–11. The mechanism of stochastic instability in the homogeneous models for classical YM fields involves the locally unstable behavior of the trajectories in phase space and is characteristic of nonlinear oscillatory systems with finitely many degrees of freedom.[12,13] Although the homogeneous YM field models are a particular case of models with inhomogeneous fields, they are still of significant interest and their properties have been discussed in detail in Refs. 7–11 for classical YM fields. Here we merely note that the homogeneous models permit extensive numerical simulations for analyzing the characteristic role of YM field nonlinearity in systems with finitely many degrees of freedom. These models also have the important property[14] that an inhomogeneous YM field cannot be integrable unless it is integrable in the homogeneous case.

We note that the condition that the field be homogeneous in fact entails the long-wavelength approximation: $\lambda \gg A^{-1}$, where λ and A are the dimensionless wavelength and the amplitude of the field.[11] We note also that it is generally a nontrivial matter to pass from homogeneous to inhomogeneous fields, because the number of degrees of freedom becomes infinite. However, various simplifications are possible even here (for instance, one can specify periodic boundary conditions,[15] in which case only finitely many modes actually contribute to the dynamics).

The energy threshold for stochastic instability depends in general on the number of degrees of freedom of the system and tends to increase with the latter. This suggests that an analysis of homogeneous models might be useful for deriving upper bounds on the energy densities corresponding to the onset of chaotic behavior in systems with nonlinear fields.

We also note that homogeneous models may play a role in the quantization of gauge fields. Since stochastic behavior implies a violation of the invariance of certain integrals of motion, one is faced with the familiar problem of determining the spectrum of the Hamiltonian even for homogeneous systems (cf. Ref. 16 and the bibliography there). In particular, examples are known of homogeneous classical YM fields for which stochastic behavior is universal, i.e., occurs for arbitrarily low energy densities (cf. Refs. 11 and 17). This implies that in these cases the quantum harmonic oscillator approximation is invalid even for low energies.

We are interested in generalizing the homogeneous models of classical YM fields so that they correspond more closely to the ones now employed in field theories. In particular, we consider how to generalize the $SU(2) \otimes U(1)$ field system in the boson long-wave sector. Analysis of this system may be useful in deriving a characteristic upper bound for the energy densities needed for onset of chaos (e.g., in quantum chromodynamics (QCD) and in electroweak interactions.

In what follows we consider the onset of random behavior in the homogeneous $SU(2) \otimes U(1)$ model with a spontaneously broken symmetry and numerically calculate the threshold energy density above which the motion becomes chaotic. We study the field dynamics and stability with respect to variations in the initial conditions, and we numerically calculate the frequency spectrum of the fields for several energy densities.

2. FUNDAMENTAL EQUATIONS

We start with the Lagrangian used in the standard Salam-Weinberg $S(U) \otimes U(1)$ model (Ref. 2), which involves only the three-color Yang-Mills boson fields A_μ^a ($a = 1, 2, 3$) and a colorless abelian field B_μ ($\hbar = c = 1$):

$$\mathcal{L} = -\frac{1}{4}\mathcal{F}_{\mu\nu}{}^a\mathcal{F}_{\mu\nu}{}^a - \frac{1}{4}G_{\mu\nu}G_{\mu\nu} + \left|\left(\partial_\mu + igS^aA_\mu{}^a + \frac{1}{2}ig_1B_\mu\right)\varphi\right|^2 - V(\varphi),$$
$$\mathcal{F}_{\mu\nu}{}^a = \partial_\mu A_\nu{}^a - \partial_\nu A_\mu{}^a + g\varepsilon^{abc}A_\mu{}^bA_\nu{}^c, \qquad G_{\mu\nu} = \partial_\mu B_\nu - \partial_\nu B_\mu. \tag{2.1}$$

The spin operators S^a are generators of the group $SU(2)$ and satisfy the commutation relations

$$[S^a, S^b] = i\varepsilon^{abc}S^c.$$

The complex field φ is the two-component Higgs field with the potential

$$V(\varphi) = -\frac{m^2}{2}\varphi^+\varphi + \lambda^2(\varphi^+\varphi)^2, \qquad \varphi = \begin{pmatrix}\varphi_1\\ \varphi_2\end{pmatrix}. \tag{2.2}$$

The Lagrangian (2.1) gives rise to the following equations of motion:

 0038-5646/85/030415-05$04.00

$$\partial^\nu G_{\mu\nu}+{}^1/_2 ig_1[(\partial_\mu\varphi^+)\varphi-\varphi^+(\partial_\mu\varphi)]+gg_1\varphi^+\mathbf{S}\mathbf{A}_\mu\varphi+{}^1/_2 g_1{}^2\varphi^+B_\mu\varphi=0, \tag{2.3}$$

$$\partial^\nu\vec{\mathcal{F}}_{\mu\nu}+g[\mathbf{A}^\nu\vec{\mathcal{F}}_{\mu\nu}]+ig[(\partial_\mu\varphi^+)\mathbf{S}\varphi-\varphi^+\mathbf{S}\partial_\mu\varphi]+{}^1/_2 g^2\varphi^+\mathbf{A}_\mu\varphi+gg_1\varphi^+\mathbf{S}B_\mu\varphi=0, \tag{2.4}$$

$$\partial_\nu\partial^\nu\varphi+V'(\varphi)+ig\mathbf{S}(\partial_\nu\mathbf{A}^\nu)\varphi+{}^1/_2 ig_1(\partial_\nu B^\nu)\varphi+2ig\mathbf{S}\mathbf{A}^\nu\partial_\nu\varphi+ig_1B^\nu(\partial_\nu\varphi)-{}^1/_4 g^2(\mathbf{A}_\nu\mathbf{A}^\nu)\varphi-gg_1\mathbf{S}\mathbf{A}_\nu B^\nu\varphi-{}^1/_4 g_1{}^2B_\nu B^\nu\varphi=0, \tag{2.5}$$

where $\mathbf{A}_\mu=(A^1_\mu, A^2_\mu, A^3_\mu)$. If the contributions from the spatial derivatives of the fields are small compared to the nonlinear terms (i.e., $gA\lambda\gg 1$, where λ is the characteristic length), we may keep only the time derivatives in the equations of motion (2.3)–(2.5). If we choose the Coulomb gauge $\mathbf{A}_0=B_0=0$, we have

$$\ddot{\mathbf{A}}_i-g^2[\mathbf{A}_k[\mathbf{A}_k\mathbf{A}_i]]+{}^1/_2 g^2\varphi^+\mathbf{A}_i\varphi+gg_1\varphi^+\mathbf{S}\varphi B_i=0, \tag{2.6}$$

$$\ddot{B}_i+gg_1\varphi^+\mathbf{S}\mathbf{A}_i\varphi+{}^1/_2 g_1{}^2\varphi^+\varphi B_i=0, \tag{2.7}$$

$$\ddot{\varphi}+V'(\varphi)+{}^1/_4 g^2\mathbf{A}_i\mathbf{A}_i\varphi+gg_1\mathbf{S}\mathbf{A}_iB_i\varphi+{}^1/_4 g_1{}^2B_iB_i\varphi=0, \tag{2.8}$$

where $i,k=1,2,3$ label the spatial components. In addition, the equations of motion (2.6)–(2.8) are supplemented by the coupling equations

$$\dot{\varphi}^+\varphi-\varphi^+\dot{\varphi}=0, \quad [\mathbf{A}_i\dot{\mathbf{A}}_i]+i(\dot{\varphi}^+\mathbf{S}\varphi-\varphi^+\mathbf{S}\dot{\varphi})=0. \tag{2.9}$$

3. THE EFFECTIVE HAMILTONIAN

The initial system consisting of Eqs. (2.6)–(2.8) and the coupling equations (2.9) can be solved conveniently in dimensionless form. Using expression (2.2) for the Higgs potential, we find from (2.6)–(2.9) that

$$d^2\mathbf{a}_i/d\tau^2+\mathbf{a}_i(\mathbf{a}_k\mathbf{a}_k)-\mathbf{a}_k(\mathbf{a}_i\mathbf{a}_k)+\Phi^+\Phi\mathbf{a}_i+4\Phi^+\mathbf{S}\Phi b_i=0, \tag{3.1}$$

$$\frac{d^2b_i}{d\tau^2}+\frac{g_1{}^2}{g^2}(\Phi^+\mathbf{S}\mathbf{a}_i\Phi+\Phi^+\Phi b_i)=0, \tag{3.2}$$

$$\frac{d^2\Phi}{d\tau^2}+\frac{4\lambda^2}{g^2}(\Phi^+\Phi-1)\Phi+\frac{1}{4}\mathbf{a}_i\mathbf{a}_i\Phi+2\mathbf{S}\Phi\mathbf{a}_ib_i+b_ib_i\Phi=0 \tag{3.3}$$

$$\left(\frac{d\Phi^+}{d\tau}\right)\Phi-\Phi^+\frac{d\Phi}{d\tau}=0, \tag{3.4}$$

$$\left[\mathbf{a}_i\frac{d\mathbf{a}_i}{d\tau}\right]+2i\left(\left(\frac{d\Phi^+}{d\tau}\right)\mathbf{S}\Phi-\Phi^+\mathbf{S}\frac{d\Phi}{d\tau}\right)=0, \tag{3.5}$$

where

$$\mathbf{a}_i=\sqrt{2}\mathbf{A}_i/r, \quad b_i=g_1B_i/\sqrt{2}rg, \quad \Phi=\varphi/r, \quad \tau=grt/\sqrt{2}, \quad r=m/2\lambda. \tag{3.6}$$

The quantity r in (3.6) is the radius of the condensed Higgs bosons.

System (3.1)–(3.5) completely specifies the dynamics of the homogeneous dimensionless fields $\mathbf{a}_i(\tau)$, $b_i(\tau)$, and $\Phi(\tau)$, which in the general case comprise 16 degrees of freedom altogether. The system of equations contains two dimensionless parameters: $\varepsilon=g_1/g=\tan(\theta)$ (where θ is the Salam-Weinberg angle), and the ratio λ/g, which determines the oscillation frequency of the Higgs field.

We will simplify the numerical analysis of Eqs. (3.1)–(3.5) by retaining only the following field components

$$a_3{}^1,\ a_3{}^2,\ a_1{}^3,\ a_2{}^3,\ b_1,\ b_2,$$

which correspond (cf. below) to two charged vector mesons ($w_{1,2}$), two neutral vector mesons ($z_{1,2}$), and two photons ($a_{1,2}$). We also choose the unitary gauge

$$\Phi^+(\tau)=(0,\ r+\theta_2(\tau)), \tag{3.7}$$

for the Higgs field[3]; the coupling equation (3.4) implies that the component $\theta_2(\tau)$ must be real-valued.

Although g_1/g is known to be ≈ 0.55 (Ref. 3), no reliable information is available for the mass of the Higgs boson, which may be assumed to lie somewhere between 7 GeV and 10^3 GeV (Refs. 3 and 4). In this paper we will take the Higgs boson to be much heavier than the vector mesons and will neglect the high-frequency Higgs oscillations $\theta_2(\tau)$. In addition, we will as usual pass to the new fields

$$a_i=(g^2+g_1{}^2)^{-1/2}(g_1b_i+ga_i{}^3), \quad w_i=a_3{}^i, \quad z_i=(g^2+g_1{}^2)^{-1/2}(gb_i-g_1a_i{}^3), \quad i=1,\ 2, \tag{3.8}$$

which describe the electromagnetic, charged vector, and neutral vector fields, respectively. In terms of the generalized coordinates $q=(a_i, w_i, z_i)$, system (3.1)–(3.3) takes the form

$$\dot{q}_s=\partial H/\partial p_s, \quad \dot{p}_s=-\partial H/\partial q_s, \quad s=1,\ldots,6, \quad p_s=(p_{a_i}, p_{w_i}, p_{z_i}) \tag{3.9}$$

which is a Hamiltonian system of equations of motion with the Hamiltonian

$$H=\frac{1}{2}\sum_{i=1,2}[\varepsilon p_a{}^2+p_w{}^2+p_{a_i}{}^2+w_i{}^2+(1+\varepsilon)z_i{}^2]+(1+\varepsilon)^{-1}[(a_1-z_1)^2+(a_2-z_2)^2](w_1{}^2+w_2{}^2), \tag{3.10}$$

where p_{a_i}, p_{w_i}, and p_{z_i} are the canonically conjugate momenta.

System (3.9) is completely equivalent to Eqs. (3.1)–(3.3) and is to be solved jointly with the coupling equation (3.5), which takes the form

$$w_1p_{w_2}-w_2p_{w_1}=0 \tag{3.11}$$

in the new variables. Since the field $\Phi(\tau)$, in (3.7) was chosen to be real, (3.4) is satisfied identically. We note that the total energy E of the system [the numerical value of the Hamiltonian H in (3.10)] is the natural parameter of the problem.

We numerically solved Eqs. (3.9) simultaneously with (3.11) in order to study how chaotic behavior develops from the dynamic motion in this system.

4. NUMERICAL RESULTS

The initial conditions for system (3.9) are not arbitrary but must satisfy the coupling equation (3.11). Moreover, (3.11) must be satisfied for all times, which provides a way of checking the computational accuracy. In our analysis of (3.9) we also used the law of energy conservation $E=\text{const}$ to monitor the accuracy. In all cases, the error in calculating E was less than 1.5%, and the coupling equation (3.11) was satisfied identically.

Local instability of the phase space trajectories is one of the criteria for stochastic motion in the system. Figure 1

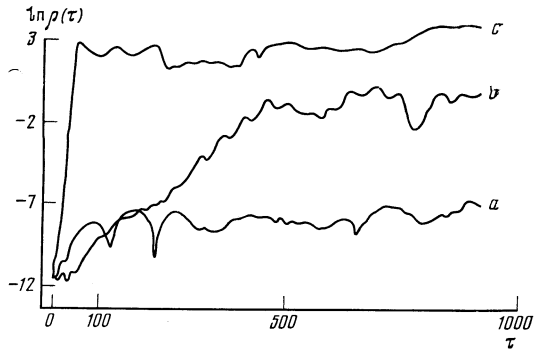

FIG. 1. Local instability of trajectories for different system energies E: a) $E = 0.03$; b) $E = 0.12$; c) $E = 5.07$ (trace c corresponds to the two trajectories in Fig. 6).

shows the typical form of the function $\ln\rho(\tau)$ for three values of E. The distance between the trajectories was calculated by the formula

$$\rho^2(\tau)=\sum_{s=1}^{6}\{[p_s^{(1)}(\tau)-p_s^{(2)}(\tau)]^2+[q_s^{(1)}(\tau)-q_s^{(2)}(\tau)]^2\}, \quad (4.1)$$

where the superscripts (1), (2) denote two trajectories with similar initial values ($\tau = 0$). The initial conditions for the trajectories in the example given below are indicated in the captions to Figs. 2 and 6. The calculations show that the function $\rho(\tau)$ starts to increase to values ~ 1 for $E \approx 0.3$. Local instability is numerically small or absent altogether for low energies $E = 0.03$–0.12, and the motion is quasiperiodic (Fig. 2a). The quasiperiodic motion of the system was the dominant feature for these energies; it was observed for all initial conditions and persisted for long characteristic times. Figure 3a shows the frequency spectrum $w_1(\omega)$ of the motion corresponding to Fig. 2a (T is the averaging time, i.e., total time interval for which the Fourier components were calculated). Figure 3a shows that the frequency spectrum $w_1(\omega)$ is highly nonlinear even for low energies and has the discrete structure characteristic of quasiperiodic motion. The characteristic frequencies for the charged vector meson w_1 lie

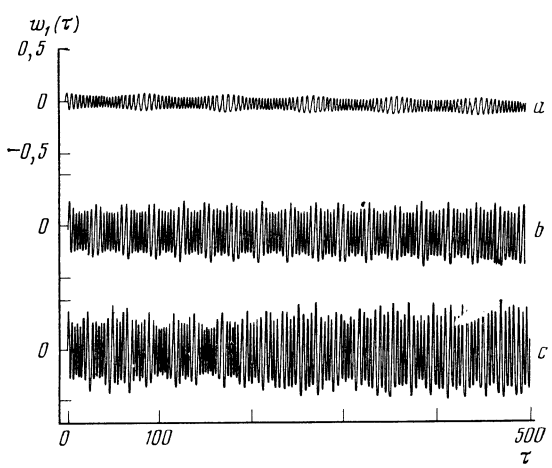

FIG. 2. Dynamics of a massive field $w_1(\tau)$ for $a_i(0) = 0.3\varepsilon^{1/2}$, $w_i(0) = z_i(0) = 0$: a) $E = 0.03$; $p_{a_i}(0) = 0.1/\sqrt{\varepsilon}$, $p_{w_i}(0) = p_{z_i}(0) = 0.1$; b) $E = 0.27$, $p_{a_i}(0) = 0.3/\sqrt{\varepsilon}$, $p_{w_i}(0) = p_{z_i}(0) = 0.3$; c) $E = 0.48$, $p_{a_i}(0) = 0.4/\sqrt{\varepsilon}$, $p_{w_i}(0) = p_{z_i}(0) = 0.4$.

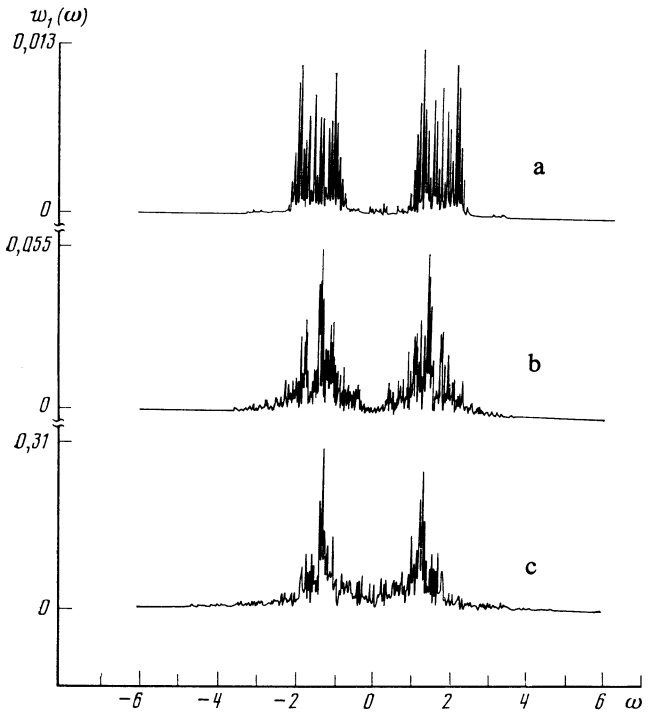

FIG. 3. Frequency spectrum $w_1(\omega)$ for the motion $w_1(\tau)$: a) $E = 0.03$; b) $E = 0.48$ (curves a, c in Fig. 2); c) $E = 5.07$ (curve a in Fig. 6).

within the frequency range found by the linear approximation: $\omega_{w_1} = 1$ [cf. (3.10)]. Most numerical analyses exploit the fact that the frequency spectrum for quasiperiodic motion is characteristically quite insensitive to increases in the computational time T (i.e., the structure of the frequency spectrum remains essentially unchanged for times T exceeding a characteristic value). This type of frequency stability was noted for low energies in our numerical simulation, and the motion of the electromagnetic field $a(\tau)$ was nearly linear for these energies (Fig. 4a; the corresponding frequency spectrum is shown in Fig. 5a). We see that the frequency is close to the value $\omega_a = 0$ given by the linear approximation.

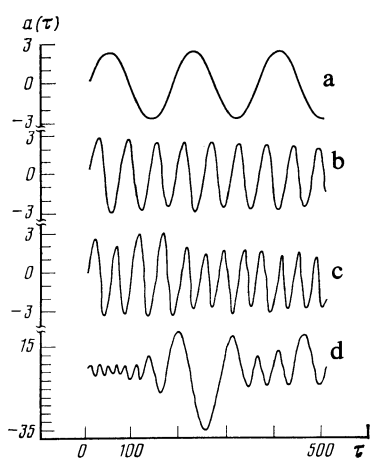

FIG. 4. Dynamics of the electromagnetic field $a(\tau) = a_1(\tau)/\varepsilon^{1/2}$: a) $E = 0.03$; b) $E = 0.27$; c) $E = 0.48$; d) $E = 5.07$.

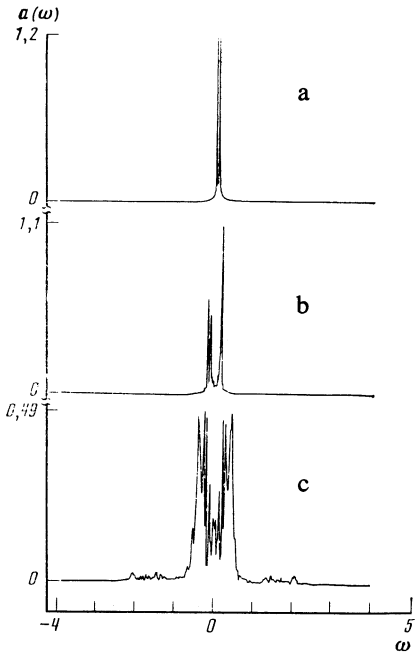

FIG. 5. Frequency spectrum $a(\omega)$ corresponding to $a(\tau)$: a) $E = 0.03$; b) $E = 0.48$; c) $E = 5.07$ (curves a, c, d in Fig. 4).

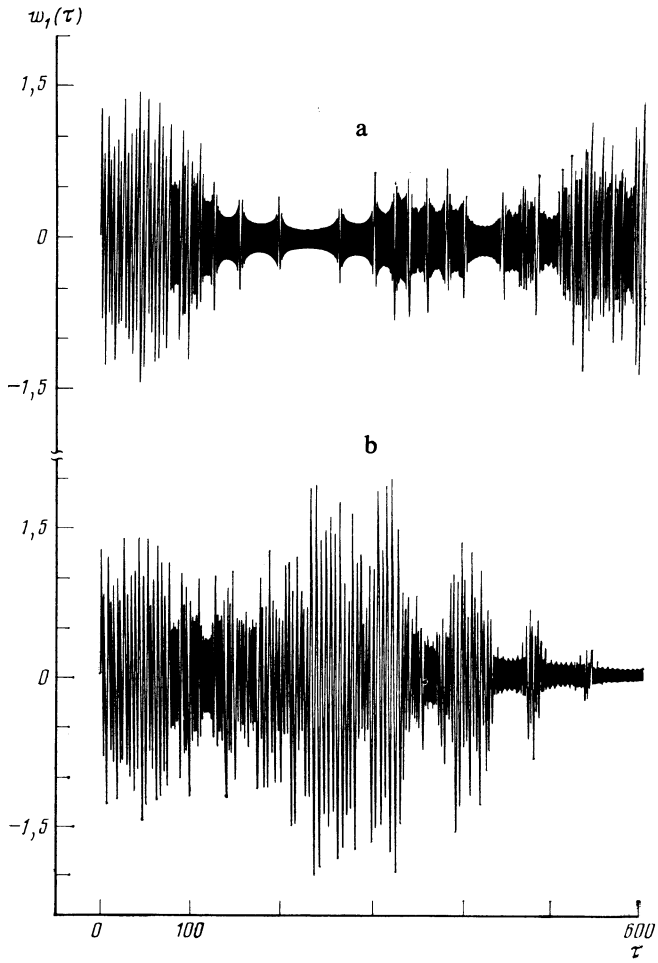

FIG. 6. Dynamics of a massive field $w_1(\tau)$ for $E = 5.07$: a) $a_1(0) = 0.3\varepsilon^{1/2}$; b) $a_1(0) = 0.300\,01\ \varepsilon^{1/2}$; the other initial conditions are the same: $a_2(0) = 0.3\ \varepsilon^{1/2}$; $w_i(0) = z_i(0) = 0$; $p_{a_i}(0) = 1.3/\varepsilon^{1/2}$; $p_{w_i}(0) = p_{z_i}(0) = 1.3$.

Irregular components of the motion are generated as E increases. Fig. 2b, c shows the irregular structure of $w_1(\tau)$ for $E \approx 0.3$, and Fig. 3b shows the corresponding spectrum $w_1(\omega)$ for $E = 0.48$. The spectral structure in this case is qualitatively different from the one in Fig. 3a and is typical of continuous spectra. The spectrum changes significantly and contains more peaks as the averaging time T is increased. Figure 4b, c plots the time dependence $a(\tau)$ of the electromagnetic field for $E = 0.03$ and 0.27; Fig. 5b shows the corresponding spectrum $a(\omega)$ for $E = 0.48$. Figure 4c shows that the electromagnetic field also contains an irregular component which causes nonlinear broadening of the spectral lines $a(\omega)$ at low frequencies.

The relative amplitude of the irregular component grows appreciably as E rises further (Fig. 4d, Fig. 6), and the local motion becomes highly unstable. The curve $\ln\rho(\tau)$ in Fig. 1c corresponds to two trajectories with nearly equal initial conditions whose motions $w_1(\tau)$ are shown in Fig. 6a, b. The difference in the initial conditions was $|\Delta a_1(0)| = 10^{-5}\varepsilon^{1/2}$. Figure 3c shows the spectrum for $w_1(\tau)$ corresponding to Fig. 6a.

The process $a_1(\tau)$ and its spectrum are shown in Fig. 4 and Fig. 5c, respectively, for the same values of E. According to Fig. 5c, the continuous component in the frequency spectrum of the electromagnetic field increases significantly with E.

5. CONCLUSIONS

The above numerical analysis shows that the transition from regular to chaotic motion occurs for energies $E \approx 0.3$. Although this value is clearly only approximate, it gives the correct order of magnitude for the energy above which the random component of the motion becomes significant. We note that threshold energies $E \sim 1$ are reasonable, because the dimensionless quantity H (3.10) is the only parameter of the system and the numerical factors are ~ 1. The numerical analysis reveals that for energies $E \approx 0.3$, the interaction energy term in the Hamiltonian (3.10) has the same order of magnitude as the energy of the noninteracting fields [the quadratic part of the Hamiltonian (3.10)]. This indicates that the nonlinearity, which is generally neglected in the standard perturbation theory, is important in the randomization process for system (2.1).

We now use the characteristic threshold energy $E \approx 0.3$ for onset of chaotic behavior in the above model to derive an order-of-magnitude estimate for the threshold in terms of the dimensional energy density $\mathscr{E}_{\text{thr}}$ for the original model with the Lagrangian (2.1). Let us estimate, e.g., the energy density contained in the field component

$$E_3^1 = -\frac{1}{c}\frac{dA_3^1}{dt}.$$

Using (3.6) and (3.8), we get the order-of-magnitude estimate

$$\mathscr{E}_{\text{thr}} = {}^1/_4 (E_3^1)^2 = {}^1/_{16} (gr^2)^2 (dw_1/d\tau)^2 = {}^1/_2 (g/G_F)^2 (dw_1/d\tau)^2 \approx 10^{50} (dw_1/d\tau)^2 \ \text{GeV/cm}^3. \quad (5.1)$$

The numerical analysis gives the estimate $(dw_1/d\tau) \sim 1/4$ for

the derivative $dw_1/d\tau$ at the threshold $E \approx 0.3$. The energy density threshold for stochastic behavior in system (2.1) is thus $\mathscr{E}_{\text{thr}} \sim 6.25 \cdot 10^{48}$ GeV/cm^3 in order of magnitude. Expression (5.1) shows that $\mathscr{E}_{\text{thr}}$ is determined primarily by the large constant factor and can probably not be significantly decreased in the electroweak theory by decreasing the threshold for stochastic behavior (e.g., by increasing the number of degrees of freedom). If we recall that the range r_{weak} of the weak forces is $\sim 3 \times 10^{-16}$ cm (Ref. 18), our upper bound for $\mathscr{E}_{\text{thr}}$ is well within the experimentally accessible range—an energy of ~ 200 GeV must be concentrated in a volume $\approx r_{\text{weak}}^3$.

Our estimate for $\mathscr{E}_{\text{thr}}$ thus gives an idea of the energy density needed for the onset of chaotic behavior in electroweak interactions. Off course, such rough estimates may differ considerably from the actual thresholds. For example, it is clear that the threshold may change significantly if the variation of the fields and their interaction with fermion fields are allowed for; in addition, quantum effects may be important.

With regard to the problem of quantizing homogeneous Hamiltonians of the type (3.10), we note that (3.10) corresponds in the quantum case to the Schrödinger operator

$$\hat{L} = -\nabla^2 + V(\mathbf{q}), \quad \mathbf{q} = (a_1, a_2, w_1, w_2, z_1, z_2), \tag{5.2}$$

which does not have a discrete spectrum. Indeed, the condition for $\hat{L}$ to have a discrete spectrum can be expressed in the form[19]

$$\inf V(\mathbf{q}) \to \infty \quad \text{for} \quad |\mathbf{q}| \to \infty. \tag{5.3}$$

The potential $V(\mathbf{q})$ in the Hamiltonian (3.10) violates (5.3) if we take $\mathbf{q} = (a_1, a_2, 0, 0, 0, 0)$; in this case $V(\mathbf{q})$ vanishes because the fields a_1, a_2 are massless. We can thus state that the homogeneous component of a massless field will always violate condition (5.3) for the associated Schrödinger operator (5.2) to have a discrete spectrum and the nature of the spectrum of $\hat{L}$ remains indeterminate in this case. The investigation of all of these matters will be important for determining the actual thresholds for stochastic behavior in modern field models.

We now pause briefly to discuss the stochastic behavior itself and the ways in which it might show up in experiments. In our above example, the oscillation frequencies in the linear approximation are $\omega_a = 0, \omega_w = 1, \omega_r = (1+\varepsilon)^{1/2}$. The spectrum of the motion will contain additional harmonics if the nonlinearity for low energies E is allowed for; in this case, the spectrum is discrete, as it should be for quasiperiodic motion. The quasiperiodicity breaks down as E increases; the frequency spectrum becomes continuous with characteristic linewidths near the frequencies given by the linear theory. Further increases in E "mix" the particles up in frequency space. This type of line broadening in the frequency spectrum is characteristic of stochastic motion,[12,13] and for massive fields it implies a random spread in the masses of the associated particles. Since stochastic behavior implies a continuous spectrum, the corresponding spread in the particle masses is also continuous. The above discussion this implies that electroweak interactions with highly nonlinear fields should give rise to a random time component of the electromagnetic field which should be detectable experimentally by standard correlation analysis.

We close by mentioning some alternative methods for treating the time-varying component of the Higgs field. We have assumed that the Higgs field is massive compared to the other fields (i.e., of higher frequency); simple estimates show that allowance for this field does not change the threshold for stochastic behavior in our case—the Higgs field is essentially involved only in the spontaneous symmetry breaking. However, if the frequency of the Higgs boson is slightly greater than or comparable to the frequencies of the other fields, it is necessary to solve system (3.1)–(3.5), including Eq. (3.3). In this case the Higgs boson may either decrease or increase the threshold E (the latter case corresponds to "stochastic pulling" of the system toward higher frequencies as a result of resonant interactions). Numerical calculations for the case when the Higgs frequency is comparable to the other field frequencies are currently in progress.

We thank D. A. Kirzhnits and I. F. Ginzburg for helpful discussions of these results.

[1]C. N. Yang and R. L. Mills, Phys. Rev. **96**, 191 (1954).
[2]A. A. Slavnov and L. D. Fadeev, Vvedenie v Kvantovuyu Teoriyu Kalibrovochnykh Polei (Introduction to the Quantum Theory of Gauge Fields), Nauka, Moscow (1978).
[3]A. A. Grib, Problemy Neinvariantnosti Vakyyma v Kvantovoi Teorii Polya, (Noninvariance of the Vacuum State in Quantum Field Theory), Atomizdat, Moscow (1978).
[4]J. C. Taylor, Gauge Theory of Weak Interactions, Cambridge Univ. Press, Cambridge (1976).
[5]N. P. Konopleva and V. N. Popov, Kalibrovochnye Polya (Gauge Fields), Atomizdat, Moscow (1980).
[6]L. B. Okun', Leptony i Kvarki (Leptons and Quarks), Nauka, Moscow (1981).
[7]G. Z. Baseyan, S. G. Matinyan, and G. K. Savvidi, Pis'ma Zh. Eksp. Teor. Fiz. **29**, 641 (1979) [JETP Lett. **29**, 587 (1979)].
[8]S. G. Matinyan, G. K. Savvidi, and N. G. Ter-Arutyunyan-Savvidi, Zh. Eksp. Teor. Fiz. **80**, 830 (1981) [Sov. Phys. JETP **53**, (1981)].
[9]S. G. Matinyan, G. K. Savvidi, and N. G. Ter-Arutyunyan-Savvidi, Pis'ma Zh. Eksp. Teor. Fiz. **34**, 613 (1981) [JETP Lett. **34**, 590 (1981)].
[10]B. V. Chirikov and D. L. Shepelyanskiĭ, Pis'ma Zh. Eksp. Teor. Fiz. **34**, 171 (1981) [JETP Lett. **34**, 163 (1981)].
[11]B. V. Chirikov and D. L. Shepelyanskiĭ, Yad. Fiz. **36**, 1563 (1982) [Sov. J. Nucl. Phys. **36**, 908 (1982)].
[12]G. M. Zaslavskiĭ and B. V. Chirikov, Usp. Fiz. Nauk **105**, 3 [Sov. Phys. Usp. **14**, 549 (1972)].
[13]B. V. Chirikov, Phys. Rep. **52**, 263 (1979).
[14]E. S. Nikolaevskiĭ and L. N. Shchur, Pis'ma Zh. Eksp. Teor. Fiz. **36**, 176 (1982) [JETP Lett. **36**, 218 (1982)].
[15]V. E. Zakharov, M. F. Ivanov, and L. N. Shchur, Pis'ma Zh. Eksp. Teor. Fiz. **30**, 39 (1979) [JETP Lett. **30**, 34 (1979)].
[16]G. M. Zaslavskiĭ, Phys. Rep. **80**, 157 (1981).
[17]J. Ford and G. H. Lunsford, Phys. Rev. **A1**, 59 (1970).
[18]N. N. Bogolyubov and D. V. Shirkov, Kvantovye Polya (Quantum Fields), Nauka, Moscow (1980), Sec. 32.5 [English translation Wiley New York (1980)].
[19]S. M. Mizohata, Theory of Partial Differential Equations [Russian translation], Mir, Moscow (1977), p. 465.

Translated by A. Mason